

# NMR Structural Elucidation of Amino Resins

A. S. Angelatos,<sup>1</sup> M. I. Burgar,<sup>2</sup> N. Dunlop,<sup>3</sup> F. Separovic<sup>1</sup>

<sup>1</sup>School of Chemistry, University of Melbourne, Melbourne, Victoria 3010, Australia

<sup>2</sup>CSIRO Materials Science & Technology, Private Bag 3, South Clayton MDC Victoria 3169, Australia

<sup>3</sup>Orica Australia Pty, Ltd. Gate 3 Ballarat Road, Deer Park, Victoria 3023, Australia

Received 7 April 2003; accepted 19 August 2003

**ABSTRACT:** Urea formaldehyde, melamine formaldehyde, and melamine urea formaldehyde (MUF) are important industrial amino resins that find application in numerous diverse areas, most notably in the bonding of wood products. To understand the physical properties of these amino resins and, hence, optimize their performance, a knowledge of their chemical structure is necessary. This article reports the use of NMR spectroscopy to acquire this information in the solid and liquid states. <sup>13</sup>C-NMR experiments, supported and augmented by <sup>1</sup>H-NMR and <sup>15</sup>N-

NMR results, showed that the two stages of resin synthesis, methylation followed by condensation, occurred in each type of resin. However, in the various MUF samples analyzed, the second step appeared to be predominantly the self-condensation of melamine and urea rather than the cocondensation of melamine and urea. © 2004 Wiley Periodicals, Inc. *J Appl Polym Sci* 91: 3504–3512, 2004

**Key words:** resins; copolymerization; structure; NMR; relaxation

## INTRODUCTION

Among the wide range of formaldehyde-based resins manufactured for use in a number of key industries, three were selected for investigation in this study: urea formaldehyde (UF), melamine formaldehyde (MF), and melamine urea formaldehyde (MUF). We report the results of a <sup>13</sup>C-NMR, <sup>15</sup>N-NMR, and <sup>1</sup>H-NMR study of these three resins done to determine the mechanism of MUF condensation.

Since the discovery in the early 1880s that the reaction of urea and formaldehyde produces a resinous material, the uses of UF resins have increased dramatically. Because of their low cost and proven performance, UF resins have become the most important wood adhesives for interior applications. However, UF-bonded wood products suffer from poor durability in high-temperature/high-humidity environments and are more prone than MF-bonded and MUF-bonded wood products to the emission of formaldehyde,<sup>1</sup> a potential source of indoor air pollution, which may lead to discomfort and/or health problems.<sup>2</sup> Both of these drawbacks result primarily from the hydrolytic instability of the cured UF resin, which in turn, is influenced by the structural moieties present in the resin.

MF resins were first introduced to the market in 1936 and today are widely used as adhesives for the

manufacture of exterior and moisture-resistant wood products. However, the advantage of higher hydrolysis resistance for MF resins is counteracted by their low storage stability in liquid form, together with their very high price.

MUF resins are commonly used as wood adhesives for both interior and exterior applications. The incorporation of melamine into UF resins improves their low water and weather resistances, consequently upgrading their performance and reducing subsequent formaldehyde emissions. However, melamine addition changes the characteristics of the UF resins (especially with regard to their reactivity), and costs increase due to the much higher price of melamine compared with urea. Accordingly, the melamine content of MUF resins is optimized to maximize hydrolytic stability and minimize costs.

The synthesis of these amino resins is essentially a two-step process:

1. Methylation: nucleophilic attack by an amino group on the electrophilic carbon of formaldehyde to form a methylol functional group.
2. Condensation: the methylols and the free precursor molecules still present in the system react to form a polymeric material.

Two mechanisms have been recognized by which condensation occurs:

1. The formation of a methylene linkage by the reaction of a methylol group with an aminic hydrogen.

Correspondence to: F. Separovic (fs@unimelb.edu.au).  
Contract grant sponsor: UniChe Scheme.

2. The formation of a dimethylene ether linkage by the reaction of two methylol groups.

There are many potentially reactive sites in the precursor molecules, and therefore, a large variety of structural moieties are possible in the amino resins, depending on the mode of preparation employed.<sup>3-6</sup> The factors that affect the composition of products include the molar ratio of the main reaction components (formaldehyde, urea, and/or melamine); the pH, temperature, and duration of the reaction; and the identities and concentrations of any other relevant substances (e.g., catalysts) present in the reaction mixture. The development of modern analytical techniques, particularly NMR spectroscopy, has facilitated the ability to determine the influence of these synthesis parameters on the resin structure.<sup>7-10</sup>

The chemical shift in a <sup>13</sup>C-NMR experiment is a sensitive probe of chemical structure, and the relatively large chemical-shift range makes <sup>13</sup>C-NMR an attractive tool for the analysis of complicated materials such as synthetic polymers and resins. Information from <sup>1</sup>H-NMR and <sup>15</sup>N-NMR can supplement <sup>13</sup>C-NMR data in the structural elucidation of amino resins. Perhaps the greatest advantage of NMR, however, lies in its ability to analyze both solid and liquid samples *in situ* without the necessity for prior modification.

In the liquid state, orientation-dependent (anisotropic) interactions are essentially averaged to zero due to rapid isotropic molecular motion; this gives rise to high-resolution spectra that contain a wealth of detailed structural information. However, liquid-state NMR techniques can be used only in the early stages of polymerization, that is, while the resin molecules still remain soluble. Limitations in the solubility of many resins, especially cured resins, can be overcome by the use of solid-state NMR with cross-polarization (CP),<sup>11</sup> the transfer of magnetization from protons to less abundant nuclei, and magic-angle spinning (MAS),<sup>12</sup> spinning the sample in a rotor at an angle of 54.7° to the magnetic field. Because molecular mobility is lower in the solid state than in the liquid state, residual anisotropic interactions, such as dipolar interactions and chemical shift anisotropy (CSA), are preserved. Hence, solid-state spectra often lack resolvable fine structure. Nevertheless, they can provide important information about internal molecular motions and dynamics and eliminate structural uncertainties associated with the dissolution process.

This article reports the use of NMR to increase our knowledge of the fundamental chemistry of amino resins and the characterization of the reaction products. Solid-state CP-MAS <sup>13</sup>C-NMR<sup>13,14</sup> was used to study the molecular structure of solid resin samples, whereas species in solution were identified with liquid-state <sup>13</sup>C-NMR, <sup>15</sup>N-NMR, and <sup>1</sup>H-NMR. The data

obtained from the one-dimensional (1D) NMR experiments was supplemented with two-dimensional (2D) heteronuclear correlation NMR experiments.

## EXPERIMENTAL

### General

UF, MF, and MUF resin samples (solid and liquid) were obtained from Orica Adhesives & Resins (Melbourne, Australia) and stored in sealed bottles at room temperature (~ 20°C). Each sample was prepared similarly to the methods described by Mercer and Pizzi<sup>15</sup> and Maylor.<sup>16</sup> A brief outline is given below of the synthetic pathway used to produce the resins, although as stated by Dunky,<sup>17</sup> the synthetic pathways are not described in detail as they are proprietary and commercially sensitive:

1. The UF resins were made with an initial formaldehyde/urea (F/U) molar ratio of 2.2; then, urea was added to bring the final F/U ratio to about 1.
2. The MF resins were made with a formaldehyde/melamine (F/M) mole ratio of about 3, and urea was added to bring the final formaldehyde/melamine and urea [(FM)/U] ratio to about 1, that is a formaldehyde/melamine/urea (F/M/U) molar ratio of about 3:1:4.
3. The MUF resins were made by the addition of urea to a low-melamine MF resin (F/M molar ratio ≈ 8); the initial (FM)/U molar ratio was about 2; then, urea was added to bring the final (FM)/U molar ratio to about 1, that is, a F/M/U molar ratio of about 8:1:9.

To determine if the melamine content influenced condensation, the melamine ratio was varied in step 3 above, so as to yield a final melamine content to total liquid resin ranging from 7 to 38% w/w. Samples were usually run within a week of preparation, other than those studied over a time course for shelf-life stability studies.

The liquid-state NMR experiments were conducted on neat resin samples and capillaries containing D<sub>2</sub>O (for locking and shimming<sup>18,19</sup>) and 3-(trimethylsilyl)proprionic acid (TMSPA, the reference standard for <sup>13</sup>C and <sup>1</sup>H chemical shifts) were inserted into the 5-mm sample tubes. Although thermally activated molecular motion generally improves spectral resolution, all of the NMR experiments were conducted under ambient conditions.

Samples for solid-state NMR analysis were prepared as described by Orica Technical Work Instruction TWI-283; namely, the liquid resins were gelled by curing at 100°C. The solid resin was then ground to a fine powder and placed in 5-mm MAS rotors.

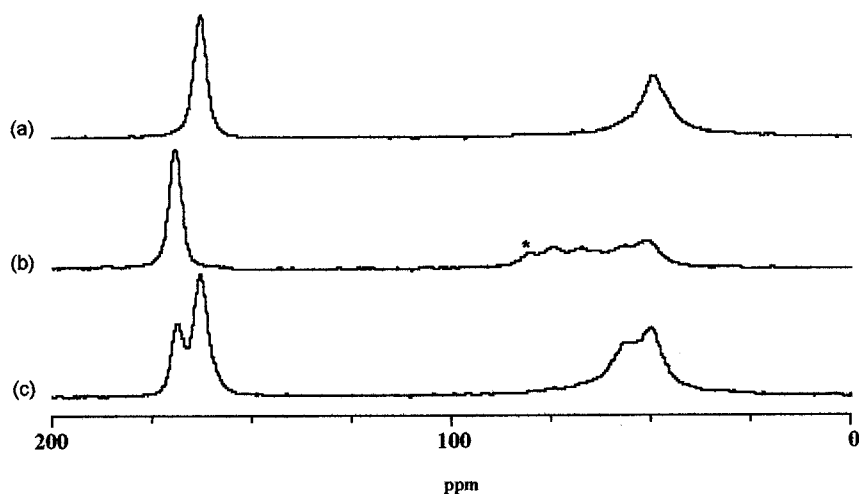


**Figure 1** Solid-state CP-MAS  $^{13}\text{C}$ -NMR spectra of amino resin samples: (a) UF, (b) MF, and (c) MUF (with  $\sim 13\%$  w/w melamine content to total liquid resin calculated, as described in the General section). The asterisk in spectrum (b) denotes a spinning side-band.

### Solid-state NMR experiments

Solid-state CP-MAS  $^{13}\text{C}$ -NMR spectra were recorded for finely ground resin samples ( $\sim 40$  mg) on a Varian (Palo Alto, CA) Inova 300 NMR spectrometer with a fixed magnetic field strength of 7.0 T. The magic angle was set by maximization of the  $^{79}\text{Br}$  spinning sidebands of KBr. Typical experimental conditions were: frequency = 75 MHz, sweep width = 30 kHz, acquisition time = 34 ms,  $90^\circ$  pulse width = 5  $\mu\text{s}$ , recycle time = 2 s, number of scans = 8700, CP contact time = 2 ms, MAS speed = 8 kHz, line broadening = 40 Hz, and external chemical shift reference = tetramethylsilane (0 ppm). At this field, the nuclear electric quadrupole effect of the  $^{14}\text{N}$  isotope<sup>8</sup> was sufficiently quenched to render adequate  $^{13}\text{C}$  resolution of adjacent carbons for accurate peak assignments.

### Liquid-state NMR experiments

Liquid-state  $^{13}\text{C}$ -NMR and  $^1\text{H}$ -NMR spectra were recorded on a Varian Inova 400 NMR spectrometer with a fixed magnetic field strength of 9.4 T. Typical experimental conditions for the proton-decoupled  $^{13}\text{C}$  spectra were: frequency = 100 MHz, sweep width = 25 kHz, acquisition time = 640 ms,  $45^\circ$  pulse width = 4  $\mu\text{s}$ , recycle time = 4 s, number of scans = 16,000, line broadening = 8 Hz, and chemical shift reference = TMSPA (0 ppm). Typical experimental conditions for the  $^1\text{H}$  spectra were: frequency = 400 MHz, sweep width = 5 kHz, acquisition time = 2 s,  $45^\circ$  pulse width = 4  $\mu\text{s}$ , recycle time = 2 s, number of scans = 16, line broadening = 0.3 Hz, chemical shift reference = TMSPA. A soft presaturation pulse was used in the  $^1\text{H}$  spectra to suppress the water resonance.<sup>20</sup>

The proton-decoupled  $^{13}\text{C}$  spectra presented here were recorded with the decoupling power on during the acquisition period *and* the delay period.  $^{13}\text{C}$  spec-

tra were also recorded with the decoupler *off* during the delay period to determine the extent of the nuclear Overhauser effect.<sup>1</sup> No discernible difference was seen between the two sets of spectra, which suggests that any signal enhancement resulting from the proton decoupling during the delay period was negligible.

Liquid-state  $^{15}\text{N}$ -NMR spectra with high-power proton decoupling were recorded on a Varian Unity Plus 400 NMR spectrometer with a fixed magnetic field strength of 9.4 T. Typical experimental conditions were: frequency = 40 MHz, sweep width = 20 kHz, acquisition time = 1 s,  $45^\circ$  pulse width = 6  $\mu\text{s}$ , recycle time = 11 s, number of scans = 10,000, line broadening = 1 Hz, and external chemical shift reference =  $\text{NH}_4^+$  ( $\text{NH}_4\text{NO}_3$ , 0 ppm).

### Analysis of data

Assignments of signals were made by comparison with the literature and relative intensity (RI) was estimated through peak integration:

1. RI is only an *approximate* measure of relative concentration as it depends on the spin-relaxation parameters of each nucleus,<sup>21</sup> and CP efficiency in the solid-state CP-MAS NMR spectra.<sup>22</sup>
2. The chemical shifts of resonances in the solid-state spectra are expressed to the nearest integer due to the line broadening associated with amorphous solids.

## RESULTS AND DISCUSSION

### Solid-state and liquid-state $^{13}\text{C}$ -NMR

$^{13}\text{C}$ -NMR spectra of the resin samples (Figs. 1 and 2) exhibited peaks in two main regions: high-field reso-

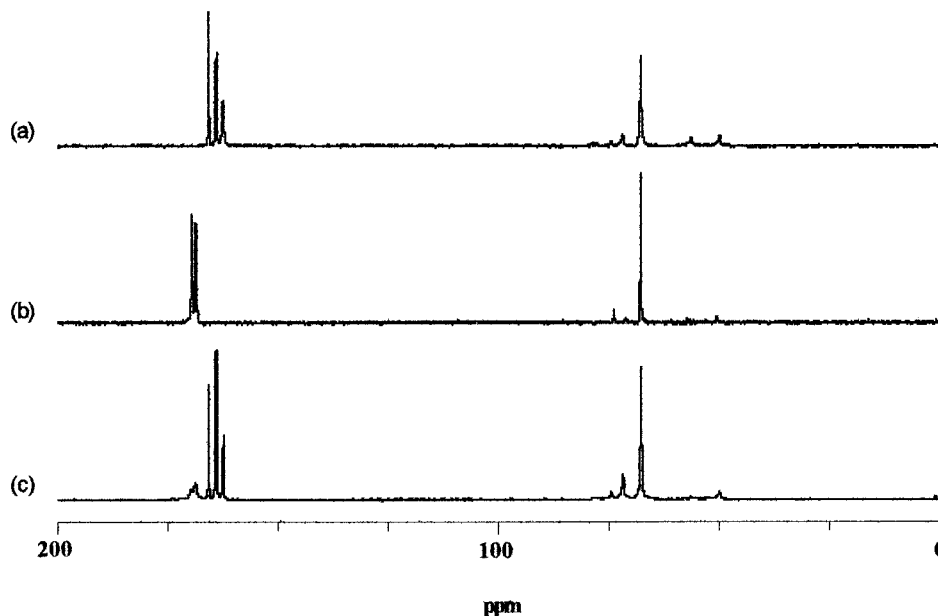


**Figure 2** Liquid-state  $^{13}\text{C}$ -NMR spectra of amino resin samples: (a) UF, (b) MF, and (c) MUF (with  $\sim 13\%$  w/w melamine).

nances (48–89 ppm) from methylene carbons in a variety of chemical environments and low-field resonances (160–170 ppm) from substituted and unsubstituted urea carbonyl carbons and/or melamine triazine carbons.

The most intense peak in the high-field region of each liquid-state spectrum (Fig. 2) arose from linear methylols, which indicated that methylation was advanced in the resin solutions. Methylol groups assist in the stability of a liquid resin; that is, they keep the polymeric molecules dissolved in the aqueous medium. Their absence could induce agglomeration, resulting in increased turbidity and reduced apparent viscosity.<sup>4</sup> In general, the methylol peaks were sharper than the methylene and dimethylene ether-linkage peaks because of higher group mobility and less variation in the environment within the polymer chain structure. For example, in the case of the liquid UF resin sample, the linewidths of the linear methylene and linear dimethylene ether-linkage signals were approximately twice that of the linear methylol signal. In addition, the UF signals were generally broader than the corresponding MF signals, which may have resulted from a larger aggregate size and, therefore, reduced dynamics at the same temperature.

Kim<sup>4</sup> reported that the migration of branched methylol groups in the lifetime of UF resins changes the chemical shifts of the neighboring methylene and dimethylene ether-linkage carbons. However, the observation of such aging effects was not the primary focus of our study. Apart from the presence of a relatively small proportion of branched methylol groups in the UF resin solution, the fact that we recorded the spectra of the sample at close intervals further precluded the observation of these spectral changes.

Just as the concentration of methylol groups serves as an indication of the extent of the methylation reaction, the amount of bridging species indicates the degree of condensation within a resin. For adhesive resins, a low degree of condensation can lead to a penetration of the resin into the wood surface that is too high, causing starved gluelines. However, high-molar-mass resins can cause insufficient wetting of the substrate surface.<sup>23</sup> Thus, the determination of the degree of condensation in resins is important.

Linear methylene bridges were relatively prominent in the high-field region of both the solid-state spectra (Fig. 1) and the liquid-state spectra (Fig. 2). Methylene linkages are desirable in resins used as wood adhesives because they are very stable to hydrolytic degradation.<sup>21</sup> Linear dimethylene ether bridges, however, were readily detected in only the liquid-state spectra (Fig. 2) because of the lack of resolution in the solid-state spectra. Although the dimethylene ether linkage is susceptible to hydrolysis, it adds elasticity to the cured resin and helps to prevent shrinkage,<sup>24</sup> which is why dimethylene ether-linked resins are an important component of foam resins used in insulation.

A moderate proportion of branched bridges may indicate that the resin will induce improved properties to composite wood panels. One might expect these units to exert a positive effect on the tensile internal bond strength of the future cured resin by acting as a nucleus for the growth of the polymer network. However, Mercer and Pizzi<sup>25</sup> proposed that branched linkages hoard the methylol groups and, therefore, disrupt the efficiency of the curing process.

There appears to be some disparity in the literature regarding whether or not cocondensation between



TABLE I  
Resonance Assignments of Solid-State CP-MAS  $^{13}\text{C}$ -NMR Spectra of  
Amino Resin Samples (Fig. 1)

| Species            | Structure   | $^{13}\text{C}$ chemical shift (ppm) |     |     |
|--------------------|---|--------------------------------------|-----|-----|
|                    |   | UF                                   | MF  | MUF |
| Linear methylene   | $-\text{NHCH}_2\text{NH}-$                                  | 48                                   | 49  | 48  |
| Branched methylene | $-\text{N}(\text{CH}_2-)\text{CH}_2\text{NH}-$              | —                                    | 55  | 55  |
| Branched methylene | $-\text{N}(\text{CH}_2-)\text{CH}_2\text{N}(\text{CH}_2-)-$ | —                                    | 62  | —   |
| Linear methylol    | $-\text{NHCH}_2\text{OH}$                                   | —                                    | 66  | —   |
| Branched methylol  | $-\text{N}(\text{CH}_2-)\text{CH}_2\text{OH}$               | —                                    | 72  | —   |
| Urea carbonyl      | $\text{>NCON}<$   | 160                                  | NA  | 161 |
| Triazine carbon    | $-\text{N}=\text{C}(\text{NR}_2)-\text{N}=-$                | NA                                   | 167 | 166 |

NA = not applicable, meaning the chemical species was not found in the resin.

melamine and urea takes place in the synthesis stage of a MUF resin. Higuchi *et al.*<sup>26</sup> asserted that cocondensation occurs exclusively in the curing process, yet Tomita and Hse<sup>27</sup> claimed to have identified signals arising from the carbons of cocondensed bridges in an uncured MUF resin. In this study, the  $^{13}\text{C}$  chemical shifts of the methylene linkages in the MUF resin were almost identical to those of the UF resin but quite different from those of the MF resin (Tables I and II). This suggested that the methylene bridges in the MUF resin arose predominantly from urea self-condensation rather than melamine and urea cocondensation, in which case, the  $^{13}\text{C}$  chemical shifts of the methylene linkages in the MUF resin would lie *between* those of the UF and MF resins. Because the  $^{13}\text{C}$  chemical shifts of the dimethylene ether linkages in the UF and MF resins were very similar (Table II), it was unclear whether the dimethylene ether bridges detected in the MUF resin arose from urea self-condensation and/or melamine self-condensation and/or melamine and

urea cocondensation. It would be reasonable to assume that the *melamine* component of a MUF resin condenses through the formation of dimethylene ether linkages in preference to methylene linkages for steric reasons.

Less intense species observed in the high-field region include methanol (found in resins made from formalin), methylene glycols (hydrated forms of free formaldehyde), and hemiformal forms of methylol groups<sup>28</sup> (transient molecules that arise from the addition of monomeric methylene glycol to methylols). These species attest to the diverse nature of the chemistry occurring in amino resins.

The low-field region of the liquid-state spectra (Fig. 2), in contrast to that of the solid-state spectra (Fig. 1), provided a good diagnostic tool for the determination of the environments around various carbonyl and triazine carbons. Relatively strong substituted peaks confirmed that methylation was advanced, even though the resin still contained free urea and/or mel-

TABLE II  
Resonance Assignments of Liquid-State  $^{13}\text{C}$ -NMR Spectra of Amino Resin Samples (Fig. 2)

| Species                              | Structure  | $^{13}\text{C}$ chemical shift (ppm) |       |       |
|--------------------------------------|--|--------------------------------------|-------|-------|
|                                      |  | UF                                   | MF    | MUF   |
| Linear methylene                     | $-\text{NHCH}_2\text{NH}-$                                 | 49.1                                 | 49.8  | 49.1  |
| Methanol                             | $\text{CH}_3\text{OH}$                                     | —                                    | —     | 51.8  |
| Branched methylene                   | $-\text{N}(\text{CH}_2-)\text{CH}_2\text{NH}-$             | 55.6                                 | —     | 55.7  |
| Linear methylol                      | $-\text{NHCH}_2\text{OH}$                                  | 67.0                                 | 67.0  | 66.8  |
| Linear dimethylene ether             | $-\text{NHCH}_2\text{OCH}_2\text{NH}-$                     | 71.1                                 | 71.0  | 71.1  |
| Linear hemiformal of methylol        | $-\text{NHCH}_2\text{OCH}_2\text{OH}$                      | 71.1                                 | 71.0  | 71.1  |
| Branched methylol                    | $-\text{N}(\text{CH}_2-)\text{CH}_2\text{OH}$              | 73.8                                 | 73.2  | 73.8  |
| Branched dimethylene ether           | $-\text{N}(\text{CH}_2-)\text{CH}_2\text{OCH}_2\text{NH}-$ | 77.5                                 | —     | —     |
| Branched hemiformal of methylol      | $-\text{N}(\text{CH}_2-)\text{CH}_2\text{OCH}_2\text{OH}$  | 77.5                                 | —     | —     |
| Monomeric methylene glycol           | $\text{HOCH}_2\text{OH}$                                   | —                                    | 84.8  | 84.9  |
| Dimeric methylene glycol             | $\text{HOCH}_2\text{OCH}_2\text{OH}$                       | —                                    | —     | 88.8  |
| <i>N,N'</i> -dimethylolurea carbonyl | $\text{HOCH}_2\text{NHCONHCH}_2\text{OH}$                  | 162.0                                | NA    | 162.0 |
| Monomethylolurea carbonyl            | $\text{H}_2\text{NCONHCH}_2\text{OH}$                      | 163.5                                | NA    | 163.5 |
| Urea carbonyl                        | $\text{H}_2\text{NCONH}_2$                                 | 165.2                                | NA    | 165.2 |
| Triazine carbon of methylolmelamines | $-\text{N}=\text{C}(\text{NR}_2)-\text{N}=-$               | NA                                   | 168.2 | 168.3 |
| Triazine carbon of melamine          | $-\text{N}=\text{C}(\text{NH}_2)-\text{N}=-$               | NA                                   | 169.1 | 169.3 |

NA = not applicable, meaning the chemical species was not found in the resin.

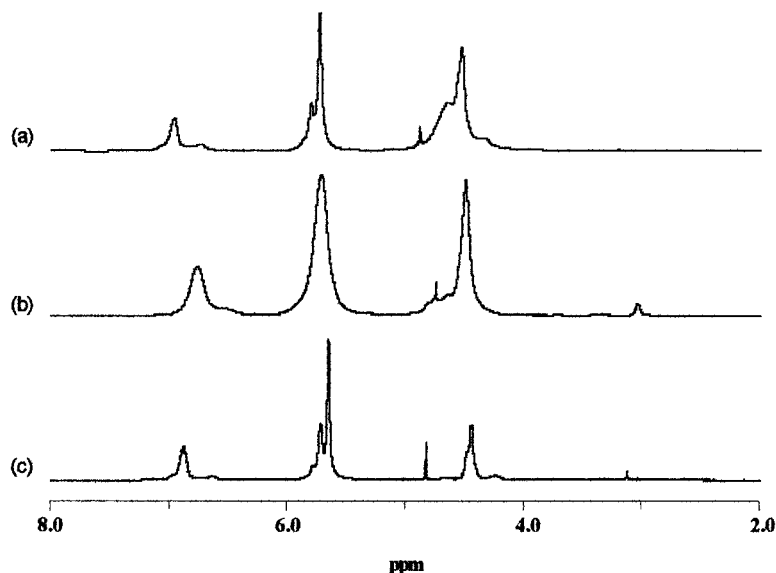


**Figure 3** Liquid-state  $^1\text{H}$ -NMR spectra (with  $\text{H}_2\text{O}$  presaturation) of amino resin samples: (a) UF, (b) MF, and (c) MUF (with  $\sim 13\%$  w/w melamine).

amine. A certain amount of unreacted material is beneficial in adhesive resins because on curing, it reacts with the free formaldehyde to form low-molecular-mass fractions that contribute to the adhesive strength at the wood-resin interface. However, an excess of unsubstituted components, at the expense of the reacted species, adversely affects the hardened resin strength.<sup>29</sup>

The absence of carbonyl signals in the 155–157 ppm region of Figure 2(a) suggested that the UF resin solution did not contain *urons*<sup>30</sup> (cyclic compounds of urea and formaldehyde). The upfield shift of uronic carbonyl signals from urea carbonyl signals is believed to be due to the steric effect of cyclization.<sup>31</sup>

### Liquid-state $^1\text{H}$ -NMR

Because of the relatively small chemical-shift range for protons and the relatively large linewidths of the  $^1\text{H}$  resonances, there was a considerable degree of signal overlap in the  $^1\text{H}$ -NMR spectra (Fig. 3). Spectral interpretation was facilitated, however, through continuous wave presaturation, a simple and effective solvent suppression technique used to attenuate the strong water resonance ( $\sim 4.8$  ppm) and, hence, reduce the dynamic range of the spectra. The structural moieties identified in the  $^1\text{H}$ -NMR spectra (Table III) were consistent with those observed in the  $^{13}\text{C}$ -NMR spectra and were useful for interpretation of the 2D  $^1\text{H}$ - $^{15}\text{N}$ -NMR spectra of the liquid resin samples (2D Liquid-State  $^1\text{H}$ - $^{15}\text{N}$ -NMR section).

### Liquid-state $^{15}\text{N}$ -NMR

The typical chemical-shift range for nitrogen resonances in polymers covers approximately 400 ppm,

which leads to a lesser likelihood of overlapping resonances than in  $^1\text{H}$ -NMR and  $^{13}\text{C}$ -NMR spectra. In addition, fewer chemically distinct types of nitrogen moieties (compared to the number of carbon moieties) in polymers result in simpler spectra and easier identification of resonances. Reluctance to use  $^{15}\text{N}$ -NMR arises from the low natural abundance and the low magnetogyric ratio of  $^{15}\text{N}$ , which in combination gives this nucleus a low receptivity. Isotopic enrichment,<sup>32–34</sup> a relatively complex and expensive procedure, is usually required, although the large-volume MAS rotor system developed by Chuang and Maciel<sup>8</sup> is a viable alternative for solid-state experiments. Because the resins analyzed in this study were rich in nitrogen, natural abundance spectra could be obtained within practical experimental time limits. A practical consequence of the high nitrogen content of amino resins is that they are nonflammable and burn only with the support of a flame.<sup>23</sup>

The liquid-state  $^{15}\text{N}$ -NMR spectrum of the MUF resin sample (Fig. 4) contained several peaks charac-

**TABLE III**  
Resonance Assignments of Liquid-State  $^1\text{H}$ -NMR Spectra of Amino Resin Samples (Fig. 3)

| Structure                  | $^1\text{H}$ chemical shift (ppm) |            |            |
|----------------------------|-----------------------------------|------------|------------|
|                            | UF                                | MF         | MUF        |
| $\text{CH}_3\text{OH}$     | 3.15                              | 3.15       | 3.15       |
| $\text{>N-CH}_2\text{-N<}$ | 4.30                              | —          | 4.25       |
| $\text{>N-CH}_2\text{-O-}$ | 4.47                              | 4.59       | 4.43, 4.45 |
| $\text{-O-CH}_2\text{-O-}$ | 4.59                              | 4.74       | 4.65       |
| Water                      | 4.83                              | 4.84       | 4.82       |
| $\text{-NH}_2$             | 5.67, 5.74                        | 5.81       | 5.65, 5.72 |
| $\text{-NH-}$              | 6.70, 6.90                        | 6.65, 6.87 | 6.65, 6.87 |

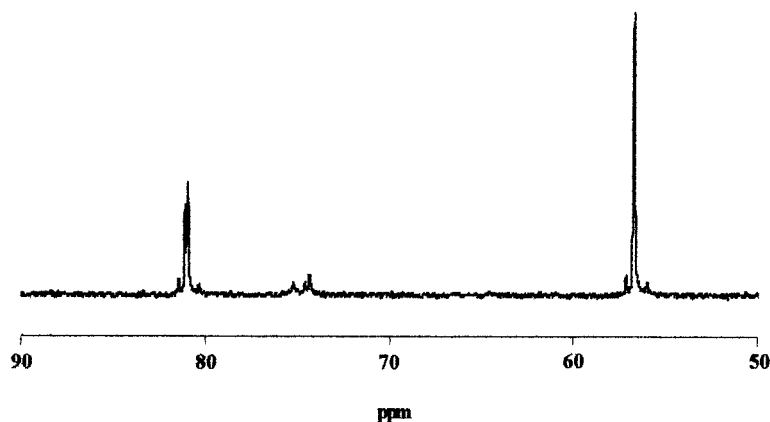


**Figure 4** Liquid-state  $^{15}\text{N}$ -NMR spectrum of the MUF resin sample (with  $\sim 13\%$  w/w melamine).

teristic of a UF system but no melamine-related signals. Two possible explanations are:

1. The melamine content of the MUF resin solution was high enough to be detected via  $^{13}\text{C}$ -NMR spectroscopy but too low to be detected via the relatively insensitive  $^{15}\text{N}$ -NMR technique.
2. The melamine component of the liquid MUF resin precipitated out of solution through condensation and/or aggregation, leaving mainly the urea component in the aqueous phase and rendering the linewidths of the melamine signals too broad for detection via liquid-state  $^{15}\text{N}$ -NMR but which were detected by solid-state CP-MAS  $^{15}\text{N}$ -NMR.

Neighboring group effects<sup>35</sup> (i.e., the effects on the positions of urea nitrogen resonances produced by the nature of the substituents attached to the geminal nitrogen) allowed the identification of some minor products, which were not observed in the relatively complicated  $^{13}\text{C}$  spectra. For example, it was possible to distinguish between linear methylene linkages within dimers and linear methylene linkages within polymer chains. By  $^{13}\text{C}$ -NMR, only linear and branched methylene bridges

were identified; the spectra gave no direct information about the location of the linkages (i.e., within dimers versus within polymers).

#### 2D liquid-state $^1\text{H}$ - $^{15}\text{N}$ -NMR

Liquid-state 2D  $^1\text{H}$ - $^{15}\text{N}$ -NMR experiments, namely, HMQC<sup>36</sup> and HMBC,<sup>37</sup> confirmed both the  $^1\text{H}$  and  $^{15}\text{N}$  NMR signal assignments proposed above (Tables III and IV). For example, the 2D  $^1\text{H}$ - $^{15}\text{N}$ -NMR spectra of the MUF resin solution contained two signals: the contours between  $\delta_{\text{N}} = 49\text{--}58$  ppm and  $\delta_{\text{H}} = 5.5\text{--}5.8$  ppm arose from primary amide groups ( $-\text{CONH}_2$ ), and those between  $\delta_{\text{N}} = 75\text{--}81$  ppm and  $\delta_{\text{H}} = 6.7\text{--}7.0$  ppm arose from secondary amide groups ( $-\text{CONH}-$ ). In both cases, the one-bond heteronuclear (N—H) scalar coupling constant was approximately 90 Hz, which is characteristic of such functional groups.<sup>38</sup>

#### $^{13}\text{C}$ -NMR of liquid MUF resins

The molar ratio of the main reaction components influences the structure of the resin produced and, in particular, the nature and extent of the condensation process. Using  $^{13}\text{C}$ -NMR spectroscopy, we investi-

**TABLE IV**  
Resonance Assignments of Liquid-State  $^{15}\text{N}$ -NMR Spectrum of the MUF Resin Sample (Fig. 4)

| Species   | Structure                                 | $^{15}\text{N}$ chemical shift (ppm) |
|---|---|--------------------------------------|
| Methylenediurea and chain ends                      | $-\text{NHCONH}_2$                        | 55.1                                 |
| Monomethylolurea                                    | $\text{H}_2\text{NCONHCH}_2\text{OH}$     | 55.8                                 |
| Urea  | $\text{H}_2\text{NCONH}_2$                | 56.2                                 |
| Linear dimethylene ether linkage within urea dimers | $-\text{NHCH}_2\text{OCH}_2\text{NH}-$    | 73.4                                 |
| Linear methylene linkage within urea polymer chains | $-\text{NHCH}_2\text{NH}-$                | 73.7                                 |
| Linear methylene linkage within urea dimers         | $-\text{NHCH}_2\text{NH}$                 | 74.3                                 |
| Chain ends  | $-\text{NHCONHCH}_2\text{OH}$             | 79.5                                 |
| $N,N'$ -dimethylolurea                              | $\text{HOCH}_2\text{NHCONHCH}_2\text{OH}$ | 80.0, 80.2                           |
| Monomethylolurea                                    | $\text{H}_2\text{NCONHCH}_2\text{OH}$     | 80.5                                 |

TABLE V  
Composition of MUF Resin Samples

| MUF resin sample | Melamine (% w/w) |          |
|------------------|------------------|----------|
|                  | Charged          | Detected |
| A                | 7                | 11       |
| B                | 10               | 14       |
| C                | 12               | 17       |
| D                | 13               | 14       |
| E                | 38               | 40       |

Melamine *charged* refers to the total mass of melamine added during synthesis relative to the final mass of liquid resin (within 1%). Melamine *detected* refers to the sum of the melamine triazine  $^{13}\text{C}$  signal intensities relative to the sum of all the  $^{13}\text{C}$  signal intensities in the spectrum of the resin solution (within 5%).

gated several MUF resin solutions with a charged melamine content (i.e., the total mass of melamine relative to the final mass of liquid resin, as described in the General section) ranging from 7 to 38% w/w.

The methylene bridges observed arose predominantly from

1. Urea self-condensation in the MUF resins containing less than 38% w/w melamine.
2. Melamine self-condensation in the MUF resin containing 38% w/w melamine.

The dimethylene ether bridges observed may have arisen from urea and/or melamine self-condensation and/or melamine and urea cocondensation. Due to the similarity in chemical shift, as discussed in the Solid-state and liquid-state  $^{13}\text{C}$ -NMR section, the different condensation pathways could not be distinguished. On the basis of the RI of these bridging structures in each sample, the MUF resin containing 38% w/w melamine exhibited a lower degree of condensation than the MUF resins containing less than 38% w/w melamine. The relatively high melamine content of this resin may have inhibited the condensation process through the aggregation of MF species. According to Jahromi,<sup>39</sup> it is the physical aggregation of MF species that limits the storage stability of a MF resin solution at room temperature (i.e., the transparent solution becomes opaque and viscosity starts to increase).

The analysis of these different MUF resin solutions also revealed that the detected melamine content (i.e., the sum of the melamine triazine  $^{13}\text{C}$  signal intensities relative to the sum of all the  $^{13}\text{C}$  signal intensities in the spectrum of the resin solution) was consistently higher than the charged melamine content (Table V). This overestimation of the melamine component may be rationalized by NMR relaxation times;<sup>40</sup> that is, melamine triazine carbons relax faster than urea car-

bonyl carbons and are, therefore, favored in a  $^{13}\text{C}$ -NMR experiment.

Several factors govern the rate at which a nucleus relaxes:

1. Dynamics: a melamine triazine carbon is generally less mobile than a urea carbonyl carbon; hence, it should recover its equilibrium properties faster after an excitation pulse.
2. Nature of the neighboring nuclei: on account of its spin quantum number ( $I = 1$ ),  $^{14}\text{N}$  possesses a nuclear electric quadrupole moment, which shortens relaxation time; a melamine triazine carbon would be more susceptible to the effects of this quadrupolar relaxation mechanism as it is directly attached to a greater number of nitrogen atoms than a urea carbonyl carbon.

To ascertain if the different relaxation times were contributing to the discrepancy in the charged and detected melamine contents, the inversion-recovery method<sup>13,14,39</sup> was employed to measure the  $T_1$  (spin-lattice or longitudinal relaxation time) of the various carbon moieties present. Average values of approximately 2.15 and 2.73 s were obtained for the melamine triazine carbons and the urea carbonyl carbons, respectively, the latter value being consistent with the 2.8 s measured by Kim and Amos<sup>1</sup> with the same method. Hence, the use of a recycle time of 4 s led to overestimation of the melamine component.

## CONCLUSIONS

Heteronuclear NMR spectroscopy was successfully applied to the analysis of amino resins. Information concerning the various structural moieties present and their relative proportions was obtained primarily from  $^{13}\text{C}$ -NMR and  $^1\text{H}$ -NMR spectra. However,  $^{15}\text{N}$ -NMR was useful in distinguishing resonances within dimers from those within polymer chains, and 2D correlation experiments eliminated the ambiguity often associated with signal assignments in 1D spectra. Cocondensation of melamine and urea through the formation of hydrolytically stable methylene linkages was not detected in this investigation. With similar industrial preparation procedures as described by Mercer and Pizzi<sup>15</sup> and Maylor,<sup>16</sup> no cocondensation was detected, whereas under certain laboratory conditions, it has been shown by Tomita and Hse<sup>41</sup> and Yanagawa et al.<sup>42</sup> that the copolymerization of MUF resins can occur. The copolymer formed by Tomita and Hse<sup>41</sup> was in the form of an oily emulsion and precipitated out of solution. Industrial applications, however, require an aqueous-based procedure, and under these conditions, crosslinking between melamine and urea was not observed. Further heteronuclear NMR experiments with  $^{15}\text{N}$ -labeled resins will be necessary to



elucidate whether or not cocondensation between melamine and urea occurs via the alternative bridging structure, namely, dimethylene ether linkages.

One of the authors (A.S.A.) gratefully acknowledges T. K. Lim (University of Melbourne) for his assistance with the operation of NMR equipment.

## References

1. Kim, M. G.; Amos, L. W. *Ind Eng Chem Res* 1990, 29, 208.
2. Guidelines for Air Quality; World Health Organization: Geneva, 2000.
3. Kim, M. G. *J Polym Sci Part A: Polym Chem* 1999, 37, 995.
4. Kim, M. G. *J Appl Polym Sci* 2000, 75, 1243.
5. Kim, M. G. *J Appl Polym Sci* 2001, 80, 2800.
6. Kim, M. G.; Wan, H.; No, B. Y.; Nieh, W. L. *J Appl Polym Sci* 2001, 82, 1155.
7. Chuang, I.; Maciel, G. E. *Macromolecules* 1992, 25, 3204.
8. Chuang, I.; Maciel, G. E. *Annu Rep NMR Spectrosc* 1994, 29, 169.
9. Rammon, R. M.; Johns, W. E.; Magnuson, J.; Dunker, A.K. *J Adhes* 1986, 19, 115.
10. Schmidt, R. G.; Ballerini, A. A.; Kamke, F. A.; Frazier, C. E. *Proc Annu Meet Adhes Soc* 1996, 19, 464.
11. Pines, A.; Gibby, M. G.; Waugh, J.S. *J Chem Phys* 1972, 56, 1776.
12. Stejskal, E. O.; Schaefer, J.; Henis, J. M. S.; Tripodi, M.K. *J Chem Phys* 1974, 61, 2351.
13. Separovic, F.; Chau, H. D.; Burgar, M. I. *Polymer* 2001, 42, 925.
14. Kishore, A. I.; Herberstein, M. E.; Craig, C. L.; Separovic, F. *Biopolymers* 2002, 61, 287.
15. Mercer, A. T.; Pizzi, A. *Holzforsch Holzverwert* 1994, 46, 51.
16. Maylor, R. *Proc Wood Adhes* 1995, 115.
17. Dunky, M. *Proc 5th Pacific Rim Bio-Based Composites Symp* 2000, 5, 205.
18. Derome, A. E. *Modern NMR Techniques for Chemistry Research*; Pergamon Press: New York, 1987.
19. Claridge, T. D. W. *High-Resolution NMR Techniques in Organic Chemistry*; Pergamon Press: New York, 1999.
20. Wider, G.; Hosur, R. V.; Wüthrich, K. *J Magn Reson* 1983, 52, 130.
21. Andreis, M.; Koenig, J. L.; Gupta, M.; Ramesh S. *J Polym Sci Part B: Polym Phys* 1995, 33, 1461.
22. Chuang I, Maciel GE. *J Appl Polym Sci* 1994, 52, 1637.
23. Dunky M. *Int J Adhes Adhes* 1998, 18, 95.
24. Meyer B, Nunlist R. *Polym Prepr* 1981, 22, 130.
25. Mercer AT, Pizzi A. *J Appl Polym Sci* 1996, 61, 1697.
26. Higuchi M, Tajima S, Irita H, Roh J, Sakata I. *Mokuzai Gakkaishi* 1991, 37, 1050.
27. Tomita B, Hse C. *Mokuzai Gakkaishi* 1995, 41, 349.
28. Tomita B, Hirose Y. *Mokuzai Gakkaishi* 1976, 22, 59.
29. Ferg EE, Pizzi A, Levendis DC. *Holzforsch Holzverwert* 1993, 45, 88.
30. Soulard C, Kamoun C, Pizzi A. *J Appl Polym Sci* 1999, 72, 277.
31. Tomita B, Hatono S. *J Polym Sci Polym Chem Ed* 1978, 16, 2509.
32. Andreis M, Koenig JL. *Adv Polym Sci* 1995, 124, 191.
33. Andreis M, Koenig JL, Gupta M, Ramesh S. *J Polym Sci Part B: Polym Phys* 1995, 33, 1449.
34. Zhou X, Frazier CE. *Int J Adhes Adhes* 2001, 21, 259.
35. Ebdon JR, Heaton PE, Huckerby TN, O'Rourke WTS, Parkin J. *Polymer* 1984, 25, 821.
36. Byrd RA, Summers MF, Zon G, Fouts CS, Marzilli LG. *J Am Chem Soc* 1986, 108, 504.
37. Summers MF, Marzilli LG, Bax A. *J Am Chem Soc* 1986, 108, 4285.
38. Martin, G. J. Martin, M. L.; Gouesnard, J.-P. *<sup>15</sup>N-NMR Spectroscopy*; Springer-Verlag: Berlin, 1981.
39. Jahromi S. *Polymer* 1999, 40, 5103.
40. Anderson WA, Freeman R, Hill H. *Pure Appl Chem* 1972, 32, 27.
41. Tomita B, Hse C. *Mokuzai Gakkaishi* 1995, 41, 490.
42. Yanagawa, R.; Mizuno, T. Sasaki, A. *Mokuzai Gakkaishi* 1962, 8, 231.